

Geological map at 1:12,500 scale of the western sector of El Hierro Island (Canary Archipelago)[☆]

Mapa geológico a escala 1:12,500 del sector occidental de la isla de El Hierro (Archipiélago Canario)

Lorenzo Poletti^a, Maria Telmon^{b,a}, Gianluca Groppelli^c, Joan Martí Molist^d, Stavros Meletlidis^e, Gianluca Norini^e, Claudia Principe^{f,g}, Andrea Di Capua^{*c}

^aUniversità degli studi di Milano – Bicocca, Milano, Italy

^bUiT The Arctic University of Norway, Tromsø, Norway

^cConsiglio Nazionale Delle Ricerche - Istituto di Geologia Ambientale e Geoingegneria, Milano, Italy

^dConsejo Superior de Investigaciones Científicas - Institut de Diagnòstic Ambiental i Estudis de l'Aigua, Barcelona, Spain

^eInstituto Geográfico Nacional, Madrid, Spain

^fConsiglio Nazionale Delle Ricerche - Istituto di Geoscienze e Georisorse, Pisa, Italy

^gIstituto Nazionale di Geofisica e Vulcanologia - Osservatorio Vesuviano, Napoli, Italy

Abstract

El Hierro, the youngest and smallest island in the Canary archipelago, has active magmatism that poses a potential hazard, evidenced by historical volcanic events such as the 1600 Lomo Negro eruption and the 2011–2012 submarine eruption off its southern coast. Despite extensive geological studies, a detailed geological map of the island was lacking until recent work. This study provides the first detailed geological map of the western sector of El Hierro (approximately 90 km²) at a 1:12,500 scale, developed from a geological survey conducted in 2022. Over 100 lava flows were identified and their directions measured, revealing stratigraphic relationships that allowed identifying formations and members and subsequently grouping them in four volcanic stages: Roque del Julan, Morro del Paso, El Jaral, and La Frontera. The study also estimates the minimum erupted volumes of over 70 lava flows. Key findings indicate that El Golfo collapse, a significant event in the island's volcanic history, led to an increased eruption frequency, but a reduction in individual eruption volumes. Additionally, the study highlights a spatial migration of eruptive fissures toward the island's outer regions post-collapse, while eruption fissure orientations remained unchanged. These findings are crucial for understanding volcanic hazards and recurrence intervals on El Hierro.

Keywords: El Hierro, geological map, lava flows, monogenetic volcanic edifices, stratigraphy, eruptive fissures

Resumen

El Hierro, la isla más joven y pequeña del archipiélago canario, tiene un magmatismo activo que representa un posible peligro, evidenciado por eventos históricos como la erupción de Lomo Negro en 1600 y la erupción submarina de 2011-2012 frente a su costa sur. A pesar de los extensos estudios geológicos, faltaba un mapa geológico detallado de la isla hasta trabajos recientes. Este estudio proporciona el primer mapa geológico detallado del sector occidental de El Hierro (aproximadamente 90 km²) a una escala de 1:12,500, desarrollado a partir de una encuesta geológica realizada en 2022. Se identificaron más de 100 flujos de lava y se midieron sus direcciones, revelando relaciones estratigráficas que permitieron identificar formaciones y miembros, y posteriormente agruparlos en cuatro etapas volcánicas: Roque del Julan, Morro del Paso, El Jaral y La Frontera. El estudio también estima los volúmenes mínimos erupcionados de más de 70 flujos de lava. Los hallazgos clave indican que el colapso de El Golfo, un evento significativo en la historia volcánica de la isla, condujo a un aumento en la frecuencia de erupciones, pero a una reducción en los volúmenes de erupción individuales. Además, el estudio destaca una migración espacial de las fisuras eruptivas hacia las regiones exteriores de la isla después del colapso, mientras que las orientaciones de las fisuras eruptivas permanecieron sin cambios. Estos hallazgos son cruciales para comprender los peligros volcánicos y los intervalos de recurrencia en El Hierro.

Palabras clave: El Hierro, mapa geológico, coladas de lava, edificios volcánicos monogenéticos, estratigrafía, fisuras eruptivas

1. Introduction

El Hierro island is the youngest, smallest, and westernmost volcanic island of the Canary archipelago, located in front of the Moroccan coastline in the Atlantic Ocean (Fig. 1). Its magmatism is still active and potentially hazardous for its inhabitants, as testified by the historical eruption of Lomo Negro on its western coast at about 1600 (Villasante-Marcos and Pavón-Carrasco, 2014; Principe et al., 2020; Risica et al., 2022) and the recent submarine eruption occurred in 2011 – 2012 offshore the southern coast, where La Restinga village is located (López et al, 2012; Pérez et al., 2014; Meletlidis et al, 2023) (Fig. 1). Although object of many geological works dealing with, for example, the reconstruction of its volcano-stratigraphy or its volcano-tectonic architectures, the island lacks a detailed geological map covering its entire surface, fundamental tool for volcanic hazard assessment, and its geology is described in a general, large-scale geological map (e.g., Carracedo et al., 2001; IGME 2010a, b, c, b; Becerril et al., 2016; León et al., 2017; Garcia-Gil et al., 2023).

To fill this gap, Abis et al. (2023) compiled the first and most detailed geological map at a scale of 1:12,500 of the southern part of El Hierro Island in 2023. In the same way, the present work documents the volcano-stratigraphic and tectonic features observed through a detailed geological survey carried out on the western sector of El Hierro island (about 90 km²) between May and July 2022 and included into a geological map at 1:12,500 scale. More than 100 lava flows were recognized, described and their flow direction measured. When possible, such lava flows were also associated with related cinder/scoria cones and eruptive fissures, whose directions were measured too. All these geological elements were then grouped into 94 formations correlated among each other based on their stratigraphic relationships observed in the field. Three main unconformities have been also identified, described and used to group the formations into 4 volcanic stages (Roque del Julian Stage, Morro del Paso Stage, El Jaral Stage and La Frontera Stage), chronologically constrained by radiometric ages available in literature. Combining lava flows areal extent and thicknesses, minimal erupted volumes have been calculated for more than 70 lava flows within the Morro del Paso, El Jaral and La Frontera Stages. In addition, density of eruptive fissures was calculated on the basis of their locations reported on the compiled geological map, eruptive fissures were plotted on a digital elevation model categorized on the basis of the associated volcanic stage and their directions of strike have been plotted in rose diagrams.

Results allow the reconstruction of the volcanological evolution of the western sector of El Hierro, indicating El Golfo

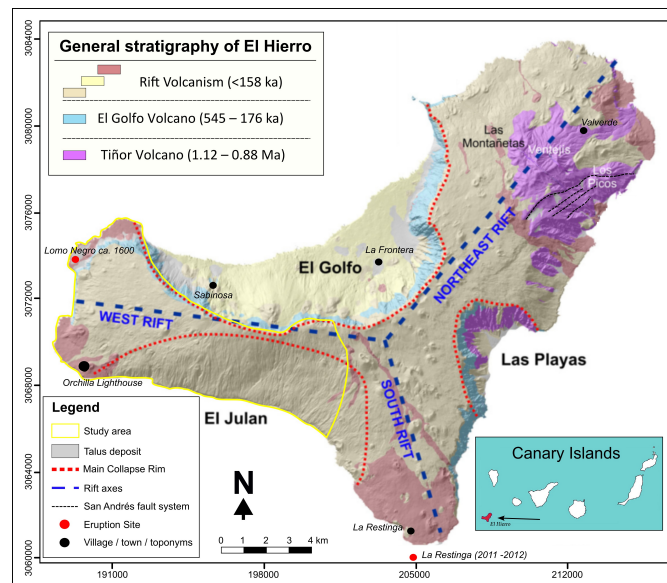


Figure 1: Simplified geological map of the El Hierro island (modified from Becerril et al., 2015) / Figura 1: Mapa geológico simplificado de la isla de El Hierro (modificado de Becerril et al., 2015).

collapse event as the cause of an increase in the frequency of eruptions for the studied sector with a concomitant decrease in their individual eruptive volume. This evidence should be taken into account when reconstructing temporal recurrences of eruptions in the area for hazard assessment purposes. Furthermore, they highlight that the location and density of the eruptive fissures shifted through time towards the edges of the volcanic island since the El Golfo collapse.

2. Geological background

The present and peculiar shape of El Hierro island (which recalls the shape of a horseshoe, hence the name) resulted from the construction and destruction of three different volcanic edifices that formed during distinct time periods and were affected by at least five lateral collapses (Fig. 1) (Masson, 1996; Carracedo et al., 1999; Gee et al., 2001; Becerril, 2014; Troll and Carracedo, 2016; León et al., 2017). The oldest edifice, El Tiñor volcano (1.12-0.88 Ma BP – Guillou et al., 1996), represents the first stage of growth of a shield volcano. At present, its remnants mainly crop out in the eastern sector of the modern island (Fig. 1) (Masson, 1996). After that, a new volcano, named El Golfo volcano (545 to 176 ka BP) (Carracedo et al., 2001), developed over the old El Tiñor edifice, filling the collapsed northwest facing flank and subsequently expanding eastwards (Carracedo et al., 2001; Troll and Carracedo, 2016). Lava flow directions indicate that this volcano was mainly constituted by a central vent close to La Frontera village, and lavas flowed radially from it along its slopes (Carracedo et al., 2001; Troll and Carracedo, 2016; León et al., 2017). According to Carracedo et al. (2001), the last eruption of the El Golfo volcano was trachytic in composition and occurred at 176 ± 3 ka BP. The last

© L. Poletti, M. Telmon, G. Groppelli, J. M. Molist, S. Meletlidis, G. Norini, C. Principe, A. Di Capua. This is an Open Access article distributed under the terms of the Creative Commons Attribution License (<https://creativecommons.org/licenses/by-nc-sa/4.0/>), which permits non-commercial sharing of the work and adaptations, provided the original work is properly cited and the new creations are licensed under identical terms.

*E-mail address: andrea.dicapua@igag.cnr.it

phase of the volcanic growth is named Rift Volcanism (since 158 ka ago) and is characterized by the activation of different eruptive fissures along the three branches of the island that lead to the formation of hundreds of cinder cones and the outflow of thin lava flows covering the island surface.

As previously mentioned, there are five main lateral collapses identified onshore and offshore the island. The first collapse probably occurred at 882 ka BP, involving the western flank of El Tiñor volcano, but no associated deposits have ever been found onshore nor offshore (Carracedo et al., 2001; Masson et al., 2002; León et al., 2017). The second collapse, named El Julan collapse, cut across the southwestern part of the edifice before 0.6 Ma BP, and its escarpment is now covered by younger lavas (Masson, 1996; Troll and Carracedo, 2016). The third and fourth collapses are called Las Playas I and Las Playas II and occurred successively at around 545 – 145 ka BP and 176 – 145 ka BP respectively (Masson et al., 2002). Together, their escarpments form the steep embayment in the southeastern side of the island (Fig. 1). The most recent collapse, called El Golfo collapse, is now considered the largest collapse occurred on the

island, and opened a large escarpment that runs from west to east for ca. 15 km, crosscutting the island from 1500 m a.s.l. down to a depth of 3200 m b.s.l. (León et al., 2017). The multiple failure generated at least a massive landslide avalanche that was first dated to an age of 17-13 ka BP (Masson, 1996; Masson et al., 1998) and then to about 120 ka BP by Carracedo et al. (2001). The most recent work by Longpré et al. (2011) fixed new constraints on El Golfo collapse and defined an age interval of 87 ± 8 ka to 39 ± 13 ka BP.

3. Methodology

A detailed field survey of an area of about 90 km² was performed at 1:10,000 scale, mapping 110 lava flows (Main Geological map and Fig. 2), and a large number of scoria and cinder cones, dykes, eruptive fissures and fault planes. The flow direction of lava flows and strike of fault planes, eruptive fissures and dykes were measured with a geological compass. Lava flows' directions were labelled as arrows on the map. Eruptive fissures

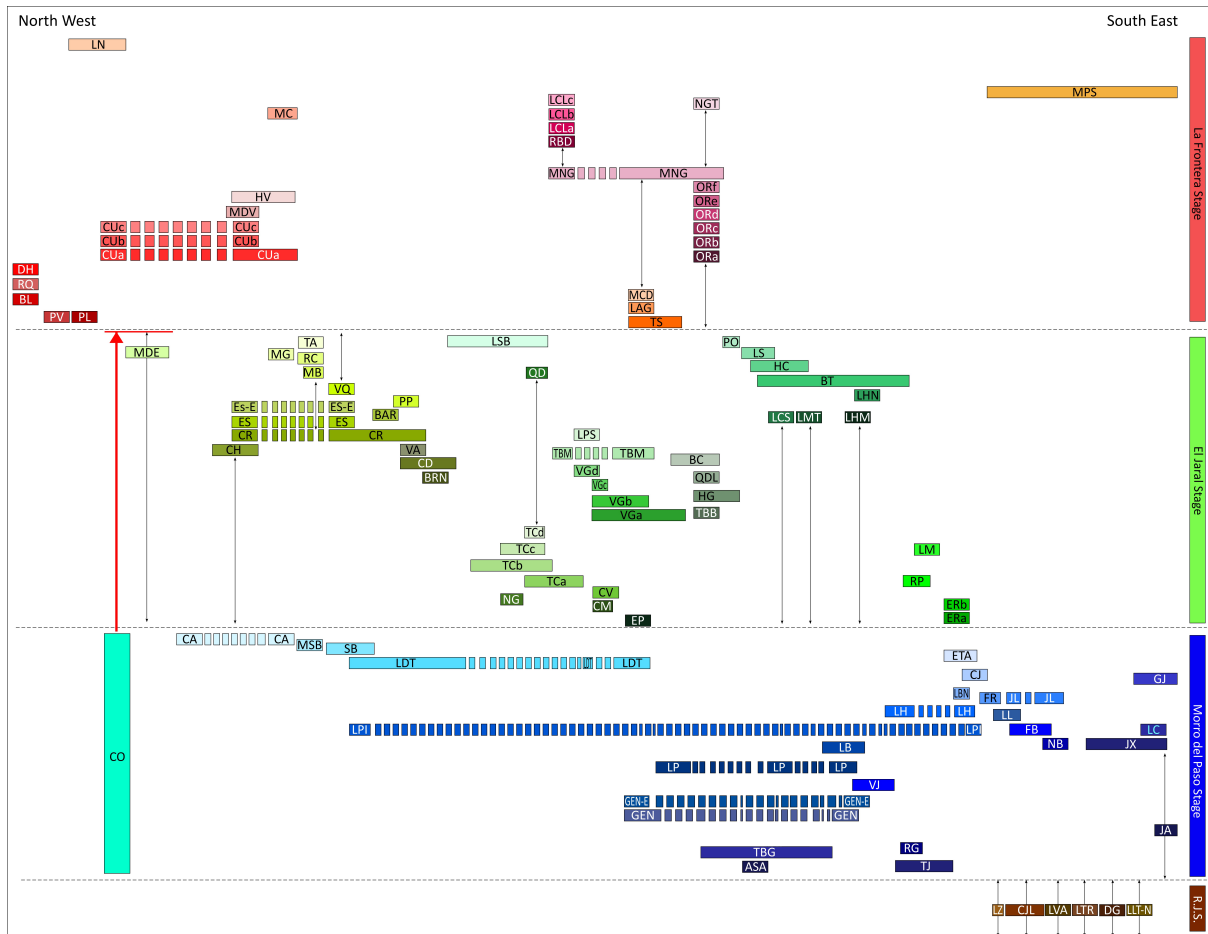


Figure 2: Stratigraphic relation scheme of the mapped formations. Black dot lines represent the boundaries of the stages. Black arrows represent the stratigraphic uncertainty, the red represents arrow the interval of deposition. Areas where formations are hidden are dashed / Figura 2: Esquema de relación estratigráfica de las formaciones mapeadas. Las líneas de puntos negras representan los límites de las etapas. Las flechas negras representan la incertidumbre estratigráfica, la flecha roja representa el intervalo de deposición. Las áreas donde las formaciones están ocultas están punteadas.

were reported on map as red dot lines, whereas faults were reported on map as continuous red line with associated kinematic over-signs. Dykes were represented by small blue lines striking their azimuth. In addition, high resolution digital elevation models (DEMs), and aerial ortho-photos were used to improve details and accuracy of the survey itself or to interpret the unsolved and inaccessible areas of the volcanic sector, such as marine cliffs and collapse escarpments.

Lava flows, cones and fallout deposits were then grouped together to form 94 informal lithostratigraphic formations (Table 1, in Suppl. Mat.), according to lithostratigraphic criteria recommended by the International Stratigraphic Guide (Salvador, 1994). Using hand specimen we have defined phenocryst abundance percentage (Porphyritic Index - P.I.), summarized in Table 1, that show a wide range of porphyritic contents among the mapped units, which are useful to distinguish in the field the mapped formations and may aid future petrographic and geochemical investigations. All the formations were named according to the site of the main outcrop and then codified. Some of these formations also include members, composed of geological bodies similar in lithology and origin, and alphabetically coded from the oldest to the youngest. Stratigraphic relationships among formations observed in the field were then summarized into the scheme of the stratigraphic relationships (Fig. 2). Age constraints of the formations, when available, were compiled from the literature (Montaña Marcos formation, C-14 – Pellicer, 1977; Golfo del Julian formation and Espigón de Los Fares formation, K-Ar – Carracedo et al., 2001; La Trinidad formation, Ar/Ar – Longpré et al., 2011; Lomo Negro formation, paleomagnetism – Villasante-Marcos et al. 2014; Member A of the Montaña Escobar formation, Ar/Ar – Becerril et al., 2016). For details, see Becerril (2014). In addition, all the often-dismantled scoria cones with an uncertain stratigraphic position - as they do not present a visible lower boundary - have been included in an informal unit, named “cones of uncertain stratigraphic position”.

The map layout and the scheme of the stratigraphic relationships (Fig. 2) were designed with the aim to provide a chronological reading criterion, with dark and stronger tones (blue, purple or dark green) for the oldest formations and in clear and bright colors for the youngest ones. With the purpose of giving an easier reading key to the map, lithofacies pattern has been added, in order to distinguish distal fallout deposits from scoria and cinder cones to related lava flow formations that have been mapped with the same color. This distinction has been obtained using the overprinting of small dots for the fallout deposits into the main Geological map.

The presence of four unconformities (two lateral collapse-related surfaces - El Julian scar and El Golfo scar - an erosional surface and a marine terrace) allowed us to identify four main stages in the construction of the western sector of the volcanic edifice and potentially the surrounding areas. At present knowledge, we cannot define synthetic units based on these unconformities because we cannot trace their lateral extension on the whole island. Therefore, the 94 formations were subsequently

grouped into 4 volcanic stages bounded by such unconformities, and named Roque del Julian Stage, Morro del Paso Stage, El Jaral Stage and La Frontera Stage (Figs. 2 and 3).

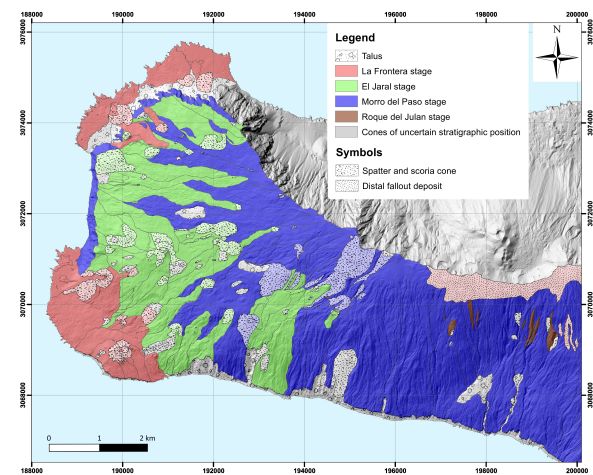


Figure 3: Map of the volcanic stages recognized in the western sector of El Hierro / Figura 3: Distribución de las etapas volcánicas as reconocidas en el sector occidental de El Hierro.

Then, volumes of lava flows belonging to the Morro del Paso Stage, the El Jaral Stage and the La Frontera Stage were compared to detect temporal changes in magma ascent rate. To obtain the minimum volume of each lava flow we multiplied the exposed area of each lava flow with the average thickness we measured in the field. The result is a minimum volume indicating an order of magnitude because of the partial exposure of lavas due to their coverage by younger lava flows and their flow into the sea. Finally, all the eruptive fissures were labelled on a digital elevation model, categorized on the basis of their stage.

4. Results and volcanological evolution

The main results on the stratigraphy, including the definition of each stage, the evolution of the western sector of El Hierro, the spatial and temporal changes in eruptive volumes, and the main volcano-tectonic trend affecting the studied area are described and discussed. All the lithostratigraphic units (member and formation ranks) are described in Table 1.

4.1. From the stratigraphy to the geological evolution of the western sector of El Hierro

The aforementioned scheme of the stratigraphic relationships (Fig. 2) and the identification of four volcanic stages including the 94 formations (Figs. 2 and 3) represent a fundamental step forward in the reconstruction of the volcanic history of the western sector of El Hierro.

The Roque del Julian stage is the oldest stage recognized in the western sector, with 9 formations emplaced after the occurrence of El Julian lateral collapse (after 0.6 Ma) (Figs. 3, 4A and 4B). Lava flows lay on El Julian collapse surface (base of the

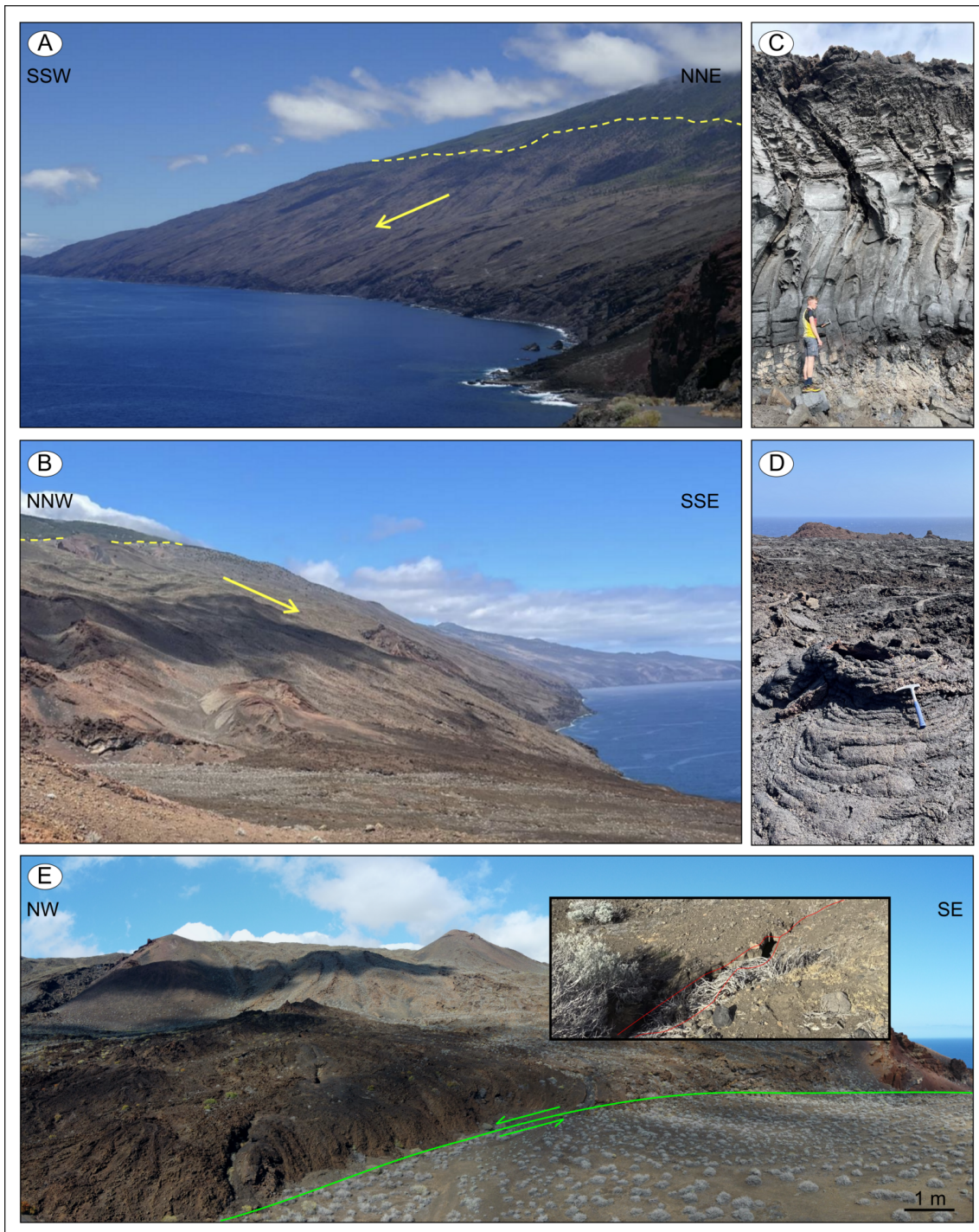


Figure 4: A) Landscape view of different lava flows included in Roque del Julian stage. The yellow dash line indicates the Julian collapse escarpment, covered by younger lava flows. The yellow arrow indicates the main flow direction. B) Landscape view showing different scoria cones included in Morro del Paso stage. The yellow dash line indicates the Julian collapse escarpment, covered by younger lava flows. The yellow arrow indicates the main flow direction. C) Section of a thick Aa flow with scoriaceous levels at the base/top and a massive layer in the middle. Dr. Poletti to scale. D) Pahoehoe lava flow field with classic ropy structures and a small hornito, where the hammer lies. E) Active fault plane mapped in the vicinity of the Orchilla lighthouse (green line – red line in the close-up view) / Figura 4: A) Vista panorámica de diferentes flujos de lava incluidos en la etapa Roque del Julian. La línea de puntos amarilla indica el escarpe de colapso de Julian, cubierto por flujos de lava más jóvenes. La flecha amarilla indica la dirección principal del flujo. B) Vista panorámica que muestra diferentes conos de escoria incluidos en la etapa Morro del Paso. La línea de puntos amarilla indica el escarpe de colapso de Julian, cubierto por flujos de lava más jóvenes. La flecha amarilla indica la dirección principal del flujo. C) Sección de un flujo Aa grueso con niveles escoriáceos en la base/cima y una capa masiva en el medio. Dr. Poletti para la escala. D) Campo de flujo de lava Pahoehoe con estructuras clásicas de cuerda y un pequeño hornito, donde se encuentra el martillo. E) Plano de falla activa mapeado en las cercanías del faro de Orchilla (línea verde – línea roja en el zoom).

stage) and are characterized by an erosional unconformity at the top, probably generated during a hiatus in volcanic activity. Due to the paucity of outcrops or their inaccessibility (steep escarpments and cliffs along the coastline), some formations were roughly described and cannot be correlated to geochronological constraints present in literature.

During the following stage, named Morro del Paso stage, thick lavas (between 5 and 70 m – Fig. 4C) belonging to 28 formations flowed mostly from eruptive vents that once were located on the volcanic sector then collapsed towards NW. For their stratigraphic positions, in this stage few lava flows erupted from vents actually located near the collapse rim were also included. In general, lava flow directions are radially distributed, so in the eastern part of the studied area, they point toward the south, with lavas homogeneously filling the depression of the El Julan lateral collapse and often covering the underlying Roque del Julan stage formations. To the west, lavas flowed towards the southwest to the west-northwest. Considering the geochronological constraints provided in literature of the youngest lava flows cut by the El Golfo escarpment, Morro del Paso stage began at ca. 115 ka and ended before ca. 39 ± 13 ka BP (Longpré et al., 2011).

El Jaral stage includes 40 formations emplaced after the El Golfo collapse multiple events and consists of thin (<15 m) pahoehoe (Fig. 4D) or pahoehoe to aa lava flows with a limited lateral extension emitted by eruptive fissures and related scoria cones almost all distributed halfway on the slope of the study area (Fig. 3). Lavas lay on top of the Morro del Paso stage formations and flowed towards the sea, being subsequently cross-cut during the formation of island cliffs. In addition, no lava attributed to this stage has been found inside El Julan engulfment.

La Frontera stage groups the youngest 19 formations of the island, including few eruptive vents with thin related lava flows that mantled the island cliffs, as well as nested vents with related thin and short lava flows partially or totally accumulated on Holocene marine terraces surrounding the island (Rodríguez-González et al., 2022) in the Orchilla, Las Calcosas, and Lomo Negro areas. Among all the lava flows, Lomo Negro formation is up to now considered the last on land eruption of El Hierro, dating back to about 1600 CE (Villasante-Marcos and Pavón-Carrasco, 2014; Risica et al. 2022). In the nearby Orchilla lighthouse, an oblique fault plane crosscutting all the recent lava flows have been recognized and mapped (Fig. 4E). This fault has left and normal components. In the northernmost part of the studied area, this stage also includes a succession of pyroclastic deposits, named Malpaso formation, erupted by the Tanganasoga center along El Golfo escarpment from 8130 ± 60 BP to 3950 ± 70 BP (Pérez Torrado et al., 2011; Pedrazzi et al., 2014).

4.2. Influence of the El Golfo Collapse on the eruptive history of the western sector of El Hierro

El Golfo Collapse event represents a turning point in the evolution of the western sector of El Hierro. Volumetric cal-

culatation performed in this work highlights that Morro del Paso stage, El Jaral stage and La Frontera stage are all characterized by some main eruptive events, anticipated and/or followed by a variable number of minor eruptions. However, minimum emitted volumes abruptly decreased from Morro del Paso stage to El Jaral and La Frontera stages, i.e. after the El Golfo Collapse, passing from a mean of ca. 0.038 km^3 per eruption to a mean of ca. 0.004 km^3 , a lower order of magnitude (Fig. 5).

This net decrease is inversely proportional to the frequency of eruptive events. Considering the collapse age constraints given by Masson (1996) and Longpré et al. (2011), Morro del Paso stage is chronologically constrained between at least ca. 115 ka (Longpré et al., 2011) and 39 ± 13 ka BP (El Golfo Collapse), meaning that 28 events occurred in at least 75 ka (ca. one event every 3 ka), whereas about 75 events occurred from 39 ± 13 ka BP until present days, giving a recurrence time of one event every ca. 500 years, so at least 6 times more frequently than before the collapse and 2 times more frequent than the time recurrence of one event every 1000 years in the southern sector of El Hierro (Abis et al., 2023). These recurrence times have statistical value and do not consider a possible clustering of volcanic activity.

Field evidence also highlighted that the opening of new eruptive fissures after El Golfo collapse progressively migrated towards the western side of the island, with those of La Frontera stage surrounding the external edges of El Hierro (Fig. 6). Such field constraints support the geophysical evidence about magma ascent pathways that have been illustrated by Martí et al. (2017) and Cabrera-Pérez et al. (2024), who highlight a progressive shift of magma batches towards the external part of El Hierro in its western side. Based on the distribution of eruptive fissure strikes, we could identify two main sectors (Fig. 7): a) in the northern sector we have fewer and most recent eruptive fissures WNW-ESE oriented, whereas b) in the southern sector the eruptive fissures belonging to three stages are WSW-ENE oriented. We did not find any eruptive fissure belonging to the Roque del Julan stage. The absence of eruptive fissures that predate El Golfo collapse in the northern sector can be explained by the lava flow resurface process or by a change in the volcano-tectonic stress field due to El Golfo flank collapse. Further studies are required in the surrounding areas.

5. Final Remarks

This work presents a new, detailed geological map (see Plate 1) at a 1:12,500 scale of the western sector of El Hierro Island, accompanied with a scheme of stratigraphic relationships, a description of each lithostratigraphic unit (Table 1), volumetric calculation of minimum eruptive rates through time and orientation data of eruptive fissures. The combination of this archive allowed to:

- Recognize four volcanic stages, name Roque del Julan stage, Morro del Paso stage, El Julan stage and La Frontera stage subdividing the entire stratigraphy on the base

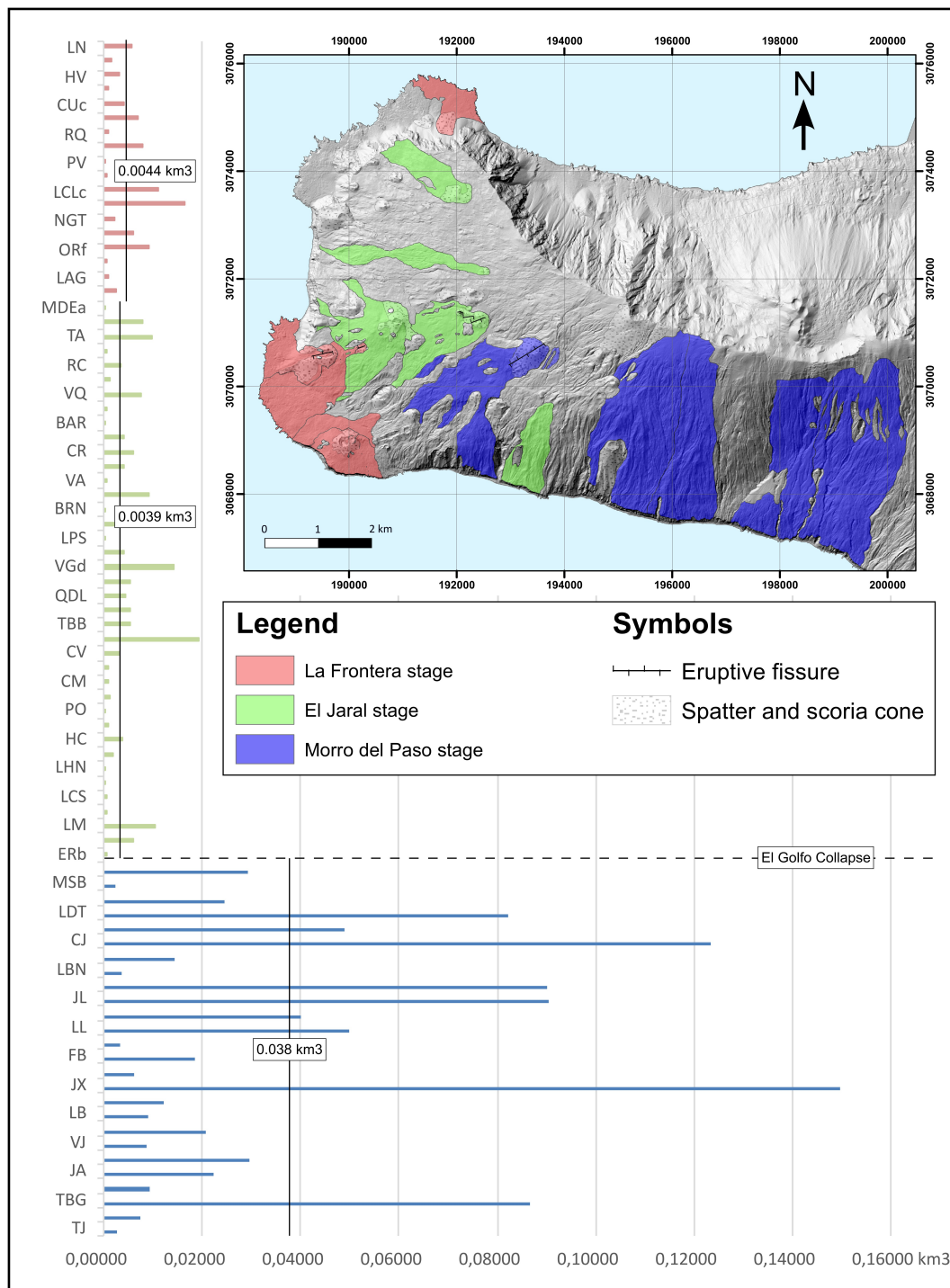


Figure 5: Erupted volumes per lava flow recognized in the field, estimated through a volume calculation using ArcGIS (for the methodology and limit, see text).

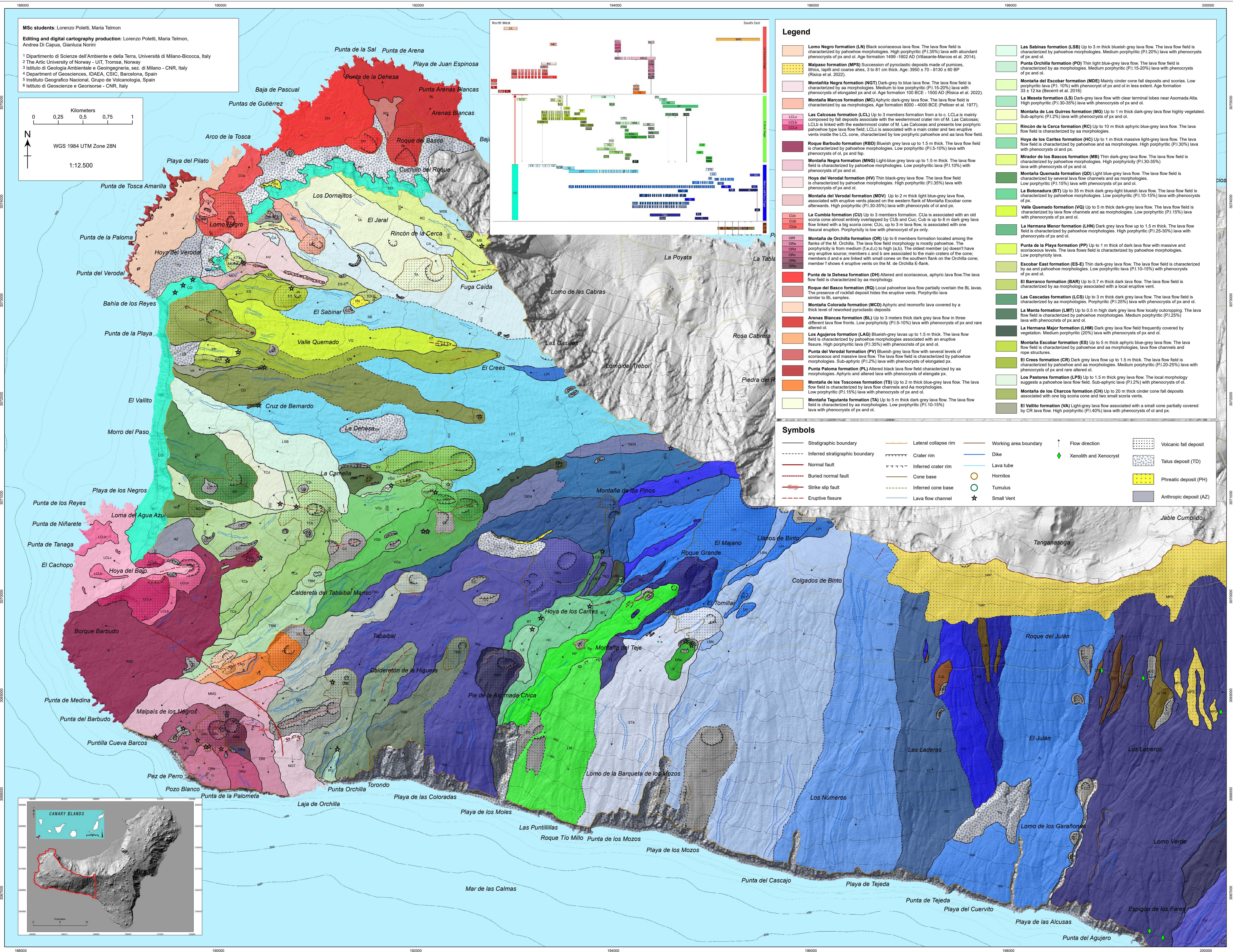
On the abscissa axis erupted volumes are plotted, on the ordinate axis lava flow names are indicated. Blue volumes are those of lavas included in the Morro del Paso stage, green volumes are those of lavas included in El Jaral stage, red volumes are those of lavas included in La Frontera stage. Vertical lines indicate mean volume calculated per stage. On the map, the five most voluminous lava flows are depicted per stage (blue = Morro del Paso stage; green = El Jaral stage; red = La Frontera stage) /

Figura 5: Volúmenes eruptivos por flujo de lava reconocidos en el campo, estimados mediante un cálculo de volumen utilizando ArcGIS (para la metodología y los límites, ver texto). En el eje de las abscisas se representan los volúmenes eruptivos, en el eje de las ordenadas se indican los nombres de los flujos de lava. Los volúmenes azules corresponden a las lavas incluidas en la etapa Morro del Paso, los volúmenes verdes corresponden a la etapa El Jaral, y los volúmenes rojos corresponden a las lavas incluidas en la etapa La Frontera. Las líneas verticales indican el volumen medio calculado por etapa. En el mapa, se representan los cinco flujos de lava más voluminosos por etapa (azul = etapa Morro del Paso; verde = etapa El Jaral; rojo = etapa La Frontera).

En el eje de las abscisas se representan los volúmenes eruptivos, en el eje de las ordenadas se indican los nombres de los flujos de lava. Los volúmenes azules corresponden a las lavas incluidas en la etapa Morro del Paso, los volúmenes verdes corresponden a la etapa El Jaral, y los volúmenes rojos corresponden a las lavas incluidas en la etapa La Frontera. Las líneas verticales indican el volumen medio calculado por etapa. En el mapa, se representan los cinco flujos de lava más voluminosos por etapa (azul = etapa Morro del Paso; verde = etapa El Jaral; rojo = etapa La Frontera).

GEOLOGY OF EL HIERRO WESTERN SECTOR (CANARY ISLAND, SPAIN)

Lorenzo Poletti¹, María Telmon^{1,2}, Gianluca GropPELLI³, Joan Martí Molist⁴, Stavros Meletlidis⁵, Gianluca Norini³, Claudia Principe⁶, Andrea Di Capua³



- Caldereta del Tabibal Manso formation (TBM)** Up to 10 m thick light blue-grey lava flow. The lava flow field is characterized by aa morphologies. Medium porphyritic (P1.20-25%) lava with phenocrysts of ol and px and presence of scoriae.
- Montaña del Barco formation (CB)** Greyish lava flow up to 2 m thick. The lava flow field is characterized by aa morphologies. Sub-aphyric (P1.13%) lava with phenocrysts of ol and rare ol.
- Cordero formation (CD)** Up to 2 m thick dark grey-blueish lava flow with associated scoriae. The lava flow field is characterized by aa morphologies.
- Cruz de Bernardo formation (BRN)** Up to 0.4 m thick dark grey lava flow. The lava flow field is characterized by pahoehoe morphologies with rope structures and hardly recognizable eruptive source. High porphyritic lava (P1.35%) with phenocrysts of ol and ol.
- Quemadillo formation (QDL)** Up to 1.5 m thick bluish dark grey lava flow. The lava flow field is characterized by aa morphologies. Medium porphyritic (P1.20%) lava with phenocrysts of ol and px.
- Calderón de la Higuera formation (HG)** Up to 2.5 m thick light-grey lava flow. The lava flow field is characterized by aa morphologies. Low porphyritic (P1.5-10%) lava with phenocrysts of ol and rare ol.
- Tabibal formation (TBB)** Up to 2 m thick blueish-grey aphyric lava flow with associated scoriae. The lava flow field is characterized by aa morphologies.
- Virgen de los Reyes formation (VG)** Up to 4 members formation. VCa is associated scoria cone; VCb and VCo are aligned on the same eruptive fissure; VGD formed an isolated cinder cone. The lava flow field is characterized by aa morphology. Porphyritic lava varies from absent (VGb) to low (VGd) and medium (VGc and VCo).
- Los Moles formation (LM)** Poorly recognizable lava flow of mixed type morphology field associated with scoriae. Medium porphyritic lava similar to LTA samples.
- Montaña Tenaca formation (TC)** Up to 4 members formation located among the flanks of the M. Tenaca. The lava flow field is characterized by aa morphologies. The porphyritic is from medium (a,b) to low (d). The oldest members (e-o) are associated to the main craters of the cone; members c and d are linked with vents on the north-eastern M. Tenaca flank.
- Roque Puguera formation (RP)** Highly scoriaceous aphyric lava flow up to 0.6 m thick. The lava flow field is characterized by aa morphology.
- Montaña de las Cuevas formation (CV)** Black-grey lava flow. The lava flow field is characterized by aa morphology and a locally peltular pre-stromatolitic level. Low porphyritic lava (P1.10%) with phenocrysts of ol and fsp.
- Pozo de los Negros formation (NG)** Up to 3 m thick dark-grey blue lava flow with scoriaceous and massive levels. The lava flow field is characterized by aa morphologies. High porphyritic (P1.30%) lava with phenocrysts of ol and ol.
- La Camella formation (CM)** Aphyric blueish-grey lava flow associated with a cinder cone and eruptive fissure. The lava flow field is characterized by aa morphologies.
- El Refugio formation (ER)** Up to 2 members formation. ERA is characterized by blueish lava associated with a scoria cone. ERB is linked with a spatter and one small hornito. The lava flow field is characterized by pahoehoe morphologies. Both ERA and ERB have medium porphyritic lava with phenocrysts of ol and ol.
- El Pastor formation (EP)** At least 1 m thick light blue-grey lava flow. The lava flow field is supposed to have an aa morphology. Low porphyritic lava (P1.5%) with phenocrysts of ol and ol.
- Fuga Calda formation (CA)** Up to 10 m thick aphyric and massive blue-grey lava flow, highly vegetated.
- Mirador de Sabinaosa formation (MSB)** Dark-grey lava flow. The lava flow field is characterized by aa morphologies. Medium porphyritic lava.
- El Sabinar formation (SB)** Dark-grey lava flow. The lava flow field is characterized by lava flow channels and aa morphologies. Sub-aphyric (P1.3%) lava with phenocrysts of ol and ol.
- El Familiar Antiguo formation (ETA)** Up to 15 m high light blue-grey lava flow associated with a big cinder cone. The lava flow field is characterized by aa morphologies, lava flow channels, tumulus and lava tubes. Porphyritic (P1.15%) lava with phenocrysts of ol.
- Lomo del Tebal formation (LDT)** Black lava flow. The lava flow field is characterized by aa morphologies. Sub-aphyric (P1.3%) lava with phenocrysts of ol and ol.
- Cascajo formation (CJ)** At least 4.5 m thick blue-grey lava flow probably associated with a collapsed scoria cone. The lava flow field is characterized by lava flow channels and aa morphologies. High porphyritic (P1.30-35%) lava with phenocrysts of ol and ol.
- Golfo de Julian formation (GJ)** Up to 25 m high light-grey lava flow. The lava flow field is characterized by lava flow channels and aa morphologies. Low porphyritic (P1.1%) lava with phenocrysts of ol and ol. Age formation 31 ± 2 ka.
- Llanos de Binto formation (LBN)** Thin, weathered and aphyric lava flow. The lava flow field is characterized by aa morphologies.
- Fuente de Rodrigo formation (FR)** Up to 7 m thick grey lava flow. The lava flow field is characterized by smooth lava flow channels and aa morphologies. High porphyritic (P1.35%) lava with phenocrysts of ol and px.
- Julan formation (JL)** Up to 60 m thick grey lava flow. The lava flow field is characterized by lava flow channels and aa morphologies. Low porphyritic lava (P1.5-10%) with phenocrysts of ol and px.
- Montaña de los Humilladeros formation (LH)** Up to 5 m thick light blue-grey lava flow. The lava flow field is characterized by aa morphologies. Low porphyritic (P1.10-15%) lava with phenocrysts of ol and px.
- Las Laderas formation (LL)** At least 2 m thick aphyric blue-grey lava flow probably associated with a collapsed scoria cone. The lava flow field is characterized by aa morphologies and lava flow channels.
- Los Picos formations (LP)** Ancient lava flows cut by El Golfo collapse escarpment.
- Fuente del Binto formation (FB)** At least 2 m thick blue-grey lava flow. The lava flow field is characterized by aa morphologies. Low porphyritic (P1.15%) lava with phenocrysts of ol and px.
- Las Caladillas formation (LC)** Up to 40 m thick light-grey lava flow. The lava flow field is characterized by lava flow channels and aa morphologies.
- La Niebla formation (NB)** Up to 6 m thick light-grey lava flow. The lava flow field is characterized by aa morphologies. Medium porphyritic (15-20%) lava with phenocrysts of ol and ol.
- Espigón de los Fares formation (JF)** Up to 30 m thick dark-grey lava flow. The lava flow field is characterized by aa morphologies. Low porphyritic (P1.10-15%) lava with phenocrysts of ol and px and xenoliths of ol up to 10 cm. Age 41 ± 2 ka.
- La Banera formation (LB)** Blue-grey lava flow associated with an eruptive vent. The lava flow field is characterized by aa morphologies. Low porphyritic lava (P1.5-10%) with phenocrysts of ol and px.
- Montaña de los Picos formation (LP)** Up to 5 m thick aphyric light blue-grey lava flow associated with two scoria cones partially eroded and collapsed.
- Venteje formation (VJ)** Up to 4 m thick blue-grey lava flow. The lava flow field is characterized by aa morphologies. Medium porphyritic (P1.20%) lava with phenocrysts of ol and ol.
- General Serrador East formation (GEN-E)** Blue-grey lava flow. The lava flow field is characterized by aa morphologies. Low porphyritic (P1.10-15%) with phenocrysts of ol and ol.
- General Serrador formation (GEN)** Blue-grey lava flow. The lava flow field is characterized by aa morphologies. Medium porphyritic (P1.20%) lava with phenocryst of ol and ol.
- Jabillo formation (JA)** Dark-grey lava flow. The lava flow field is characterized by aa morphologies. Low porphyritic (P1.5-10%) lava with phenocrysts of ol.
- Roque Grande formation (RG)** Up to 4 m thick cinder cone fall deposit associated with a big scoria cone.
- Montaña Tembaranga formation (TRB)** Up to 30 m thick blue-grey lava flow. The lava flow field is characterized by lava flow channels and aa morphologies. Medium porphyritic (P1.25%) lava with phenocrysts of ol, ol and fsp.
- Montaña Asomada Alta formation (ASA)** Up to 20 m thick dark blue-grey lava flow and fall deposit associated with a big collapsed cinder cone. Medium porphyritic (P1.20%) lava with phenocrysts of ol and ol.
- Montaña del Teje formation (TJ)** Light blue-grey lava associated with a collapsed scoria cone. The lava flow field is characterized by lava flow channels and aa morphologies. Medium porphyritic (P1.20%) lava with phenocrysts of ol and ol.
- El Comandante formation (CO)** Succession made of thick, often parallel lava flows locally interbedded with scoria, spatter and tuff cones. Porphyritic lava (P1.10-20%) with phenocrysts of ol and ol of variable in size and quantity.
- La Mazorca formation (LZ)** Lava flow partially covered by younger formations. High porphyritic (P1.30%) lava with phenocrysts of ol and ol.
- Camino del Julian formation (CJL)** Ancient lava flow field characterized by aa morphologies. Medium porphyritic (P1.15-20%) lava with phenocryst of ol and px.
- Los Valles formation (LVA)** Up to 4m thick lava flow. The lava flow field is characterized by aa morphologies. Low porphyritic (P1.5%) lava with phenocrysts of ol.
- La Trinidad formation (LTR)** Ancient lava flow partially covered by younger formations. High porphyritic (P1.35-40%) lava with phenocrysts of ol and px.
- Dos Golpes formation (DG)** Up to 3 m thick lava flow. The lava flow field is characterized by aa morphologies. Low porphyritic (P1.5%) lava with phenocrysts of ol and ol.
- Los Letreros North formation (LLT-N)** Up to 18 m thick lava flow. The lava flow field is characterized by aa morphologies. Low porphyritic (P1.10-15%) with phenocrysts and xenocrysts of ol and ol.
- Cones of uncertain stratigraphic position (CC)** Ancient scoria and spatter cones with associated heterometric deposits.

of the presence of stratigraphic elements such as unconformities. This represents the first attempt to subdivide the stratigraphy of El Hierro in stratigraphically based groups and will be of utmost importance in the reconstruction of the geology of the entire island and also useful moving to synthetic units.

- Define the impact that El Golfo collapse had on eruptive rates and frequency in the western sector of the island, with a net decrease of erupted volume per event in the face of a net increase in eruption frequency. This result greatly improves our understanding of the island’s evolution, magma batch’s locations, and directly impact the hazard assessment of this island sector.
- Identify that the orientations of eruptive fissures change spatially (northern and southern sectors), accompanied by a progressive shift of the opening of eruptive fissures towards the western edges of this sector, as shown also in fig. 6.

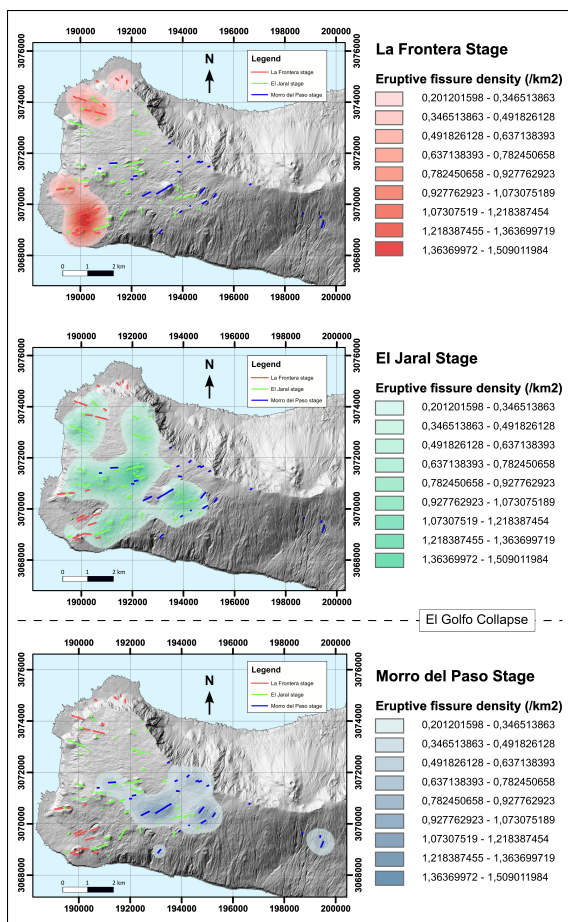


Figure 6: eruptive fissures’ density subdivided into volcanic stages. Please note the progressive shifting of fissures’ locations towards the western edges of the island / Figura 6: densidad de las fisuras eruptivas subdividida en etapas volcánicas. Tenga en cuenta el cambio progresivo de la ubicación de las fisuras hacia los ramales occidentales de la isla.

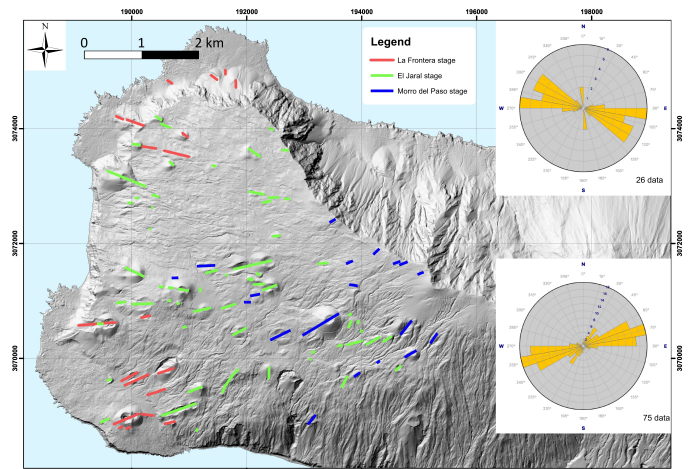


Figure 7: eruptive fissures’ orientation for Morro del Paso, El Jiral and La Frontera stages. Rose diagrams refer to the orientation of the fissures in the northern (upper diagram) and southern (lower diagram) sectors of the investigated area / Figura 7: orientación de las fisuras eruptivas para las etapas de Morro del Paso, El Jiral y La Frontera. Los diagramas de rosa se refieren a la orientación de las fisuras en el norte (diagrama superior) y en el sur (diagrama inferior) del área investigada.

Software

The geological features have been digitized and labelled into a geological map realized using ArcGIS Desktop 10.6 Software by ESRI. The base layer of the map consists in a 5 m pixel-sized LIDAR Digital Elevation Model and the topographic maps of the Mapa Topográfico Nacional 1:25.000 de España (<https://www.idee.es/csw-inspire-idee/srv/spa/catalog.search?#/metadata/spainMTN25VectorSerie>). Structural data were analyzed using ArcGIS Desktop 10.6 Software by ESRI and TectonicFP. The final design of the map has been made in Adobe Illustrator software.

Acknowledgments and funding

The authors acknowledge Emanuela De Beni and Marie-Noëlle Guilbaud for their fruitful reviews. Marc-Anointe Longpré is acknowledged for supplying thin section microphotographs and related descriptions of dated lava flow samples included in his article.

Declaration of interest statement

No potential conflict of interest was reported by the authors.

Data availability statement

The geographical data that support the geological map are freely available at <http://centrodedescargas.cnig.es/>

[CentroDescargas/index.jsp](#); the geological data that support the findings of this study are available from the corresponding author upon reasonable request. You can download the layers (*.shp,*.tif) of the final map from the journal's Spatial Data Infrastructure (SDI) and from the Interactive map interface.

References

- Abis, C., Dajma, F., Di Capua, A., Martí Molist, J., Meletlidis, S., Norini, G., Principe, C., Gropelli, G., 2023. Geology of El Hierro Southern Rift, Canary Islands, Spain. *Journal of Maps* 19 (1), 2214173, <https://doi.org/10.1080/17445647.2023.2214173>.
- Becerril, L., 2014. Volcano-structural study and long-term volcanic hazard assessment on El Hierro Island (Canary Islands). [PhD thesis, Universidad de Zaragoza, 290 pp.].
- Becerril, L., Galindo, I., Martí, J., Gudmundsson, A., 2015. Three-armed rifts or masked radial pattern of eruptive fissures? The intriguing case of El Hierro volcano (Canary Islands). *Tectonophysics* 647-648, 33–47, <https://doi.org/10.1016/j.tecto.2015.02.006>.
- Becerril, L., Galve, J., Morales, J., Romero, C., Sánchez, N., Martí, J., Galindo, I., 2016. Volcano-structure of El Hierro (Canary Islands). *Journal of Maps* 12 (sup1), 43–52, <https://doi.org/10.1080/17445647.2016.1157767>.
- Cabrera-Pérez, I., Soubestre, J., D'Auria, L., Przeor, M., García, R., Barrancos, J., Padilla, G. D., Pérez, N. M., Prudencio, J., 2024. Ambient noise tomography of El Hierro island (Canary Islands). *Frontiers in Earth Science* 11, <https://doi.org/10.3389/feart.2023.1326634>.
- Carracedo, J. C., Badiola, E. R., Guillou, H., Nuez, J. d. I., Torrado, F. J. P., 2001. Geology and volcanology of La Palma and El Hierro, Western Canaries. *Estudios Geológicos* 57 (5-6), 175–273, <https://doi.org/10.3989/egool.01575-6134>.
- Carracedo, J. C., Day, S. J., Guillou, H., Pérez Torrado, F. J., 1999. Giant Quaternary landslides in the evolution of La Palma and El Hierro, Canary Islands. *Journal of Volcanology and Geothermal Research* 94 (1), 169–190, [https://doi.org/10.1016/S0377-0273\(99\)00102-X](https://doi.org/10.1016/S0377-0273(99)00102-X).
- Carracedo, J.-C., Perez-Torrado, F.-J., Rodriguez-Gonzalez, A., Fernandez-Turiel, J.-L., Klügel, A., Troll, V. R., Wiesmaier, S., 2012. The ongoing volcanic eruption of El Hierro, Canary Islands. *Eos, Transactions American Geophysical Union* 93 (9), 89–90, <https://doi.org/10.1029/2012EO090002>.
- García-Gil, A., Baquedano, C., Marazueta, M. A., Martínez-León, J., Cruz-Pérez, N., Hernández-Gutiérrez, L. E., Santamarta, J. C., 2023. A 3D geological model of El Hierro volcanic island reflecting intraplate volcanism cycles. *Groundwater for Sustainable Development* 21, 100936, <https://doi.org/10.1016/j.gsd.2023.100936>.
- Guillou, H., Carracedo, J. C., Torrado, F. P., Badiola, E. R., 1996. K-Ar ages and magnetic stratigraphy of a hotspot-induced, fast grown oceanic island: El Hierro, Canary Islands. *Journal of Volcanology and Geothermal Research* 73 (1), 141–155, [https://doi.org/10.1016/0377-0273\(96\)00021-2](https://doi.org/10.1016/0377-0273(96)00021-2).
- IGME, 2010a. Mapa Geológico de España, Escala 1:25.000. Isla de El Hierro. Hoja 1105-II, Valverde. 96 pp.
- IGME, 2010b. Mapa Geológico de España, Escala 1:25.000. Isla de El Hierro. Hoja 1105-III, Sabinosa. 71 pp.
- IGME, 2010c. Mapa Geológico de España, Escala 1:25.000. Isla de El Hierro. Hoja 1105-IV, Frontera. 84 pp.
- IGME, 2010d. Mapa Geológico de España, Escala 1:25.000. Isla de El Hierro. Hoja 1108-I/II, La Restinga. 55 pp.
- León, R., Somoza, L., Urgeles, R., Medialdea, T., Ferrer, M., Biain, A., García-Crespo, J., Mediato, J. F., Galindo, I., Yepes, J., González, F. J., Gimenez-Moreno, J., 2017. Multi-event oceanic island landslides: New onshore-offshore insights from El Hierro Island, Canary Archipelago. *Marine Geology* 393, 156–175, <https://doi.org/10.1016/j.margeo.2016.07.001>.
- Longpré, M.-A., Chadwick, J. P., Wijbrans, J., Iping, R., 2011. Age of the El Golfo debris avalanche, El Hierro (Canary Islands): New constraints from laser and furnace $^{40}\text{Ar}/^{39}\text{Ar}$ dating. *Journal of Volcanology and Geothermal Research* 203 (1), 76–80, <https://doi.org/10.1016/j.jvolgeores.2011.04.002>.
- López, C., Blanco, M. J., Abella, R., Brenes, B., Cabrera Rodríguez, V. M., Casas, B., Domínguez Cerdeña, I., Felpeto, A., de Villalta, M. F., del Fresno, C., García, O., García-Arias, M. J., García-Cañada, L., Gomis Moreno, A., González-Alonso, E., Guzmán Pérez, J., Iribarren, I., López-Díaz, R., Luengo-Oroz, N., Meletlidis, S., Moreno, M., Moure, D., de Pablo, J. P., Rodero, C., Romero, E., Sainz-Maza, S., Sente Domingo, M. A., Torres, P. A., Trigo, P., Villasante-Marcos, V., 2012. Monitoring the volcanic unrest of El Hierro (Canary Islands) before the onset of the 2011–2012 submarine eruption. *Geophysical Research Letters* 39 (13), <https://doi.org/10.1029/2012GL051846>.
- Martí, J., Villaseñor, A., Geyer, A., López, C., Tryggvason, A., 2017. Stress barriers controlling lateral migration of magma revealed by seismic tomography. *Scientific Reports* 7 (1), 40757, <https://doi.org/10.1038/srep40757>.
- Masson, D. G., 1996. Catastrophic collapse of the volcanic island of Hierro 15 ka ago and the history of landslides in the Canary Islands. *Geology* 24 (3), 231–234, [https://doi.org/10.1130/0091-7613\(1996\)024<0231:CCOTVI>2.3.CO;2](https://doi.org/10.1130/0091-7613(1996)024<0231:CCOTVI>2.3.CO;2).
- Masson, D. G., Canals, Alonso, Urgeles, Huhnerbach, 1998. The Canary Debris Flow: source area morphology and failure mechanisms. *Sedimentology* 45 (2), 411–432, <https://doi.org/10.1046/j.1365-3091.1998.0165f.x>.
- Masson, D. G., Watts, A. B., Gee, M. J. R., Urgeles, R., Mitchell, N. C., Le Bas, T. P., Canals, M., 2002. Slope failures on the flanks of the western Canary Islands. *Earth-Science Reviews* 57 (1), 1–35, [https://doi.org/10.1016/S0012-8252\(01\)00069-1](https://doi.org/10.1016/S0012-8252(01)00069-1).
- Meletlidis, S., Becerril, L., Felpeto, A., 2023. Past, Present and Future Volcanic Activity on El Hierro. En: González, P. J. (Ed.), *El Hierro Island*. Springer International Publishing, Cham, pp. 17–39, https://doi.org/10.1007/978-3-031-35135-8_2.
- Pellicer Bautista, M. J., 1977. Estudio volcánológico de la Isla de El Hierro (Islas Canarias). *Estudios geológicos* 33 (2), 181.
- Perez-Torrado, F. J., Rodriguez-Gonzalez, A., Carracedo, J. C., Fernandez-Turiel, J. L., Guillou, H., Hansen, A., Rodriguez Badiola, E., 2011. Edades C-14 del Rift ONO de El Hierro (Islas Canarias) Presented at the El Cuaternario en España y Áreas Afines, Avances en 2011, Asociación Española para el Estudio del Cuaternario (AEQUA), pp. 101-104.
- Principe, C., Meletlidis, S., Giordano, D., Kolzenburg, S., La Felice, S., Gogichaishvili, A., Devidze, M., Cejudo, R., Gropelli, G., Dingwell, D., Martí Molist, J., 2020. Lomo Negro (El Hierro)—geology, archaeomagnetic dating and emplacement dynamics of a “monogenetic” eruption. IAVCEI8th International Maar Conference.
- Risica, G., Di Roberto, A., Speranza, F., Carlo, P. D., Pompilio, M., Meletlidis, S., Todrani, A., 2022. Reconstruction of the subaerial Holocene volcanic activity through paleomagnetic and ^{14}C dating methods: El Hierro (Canary Islands). *Journal of Volcanology and Geothermal Research* 425, 107526, <https://doi.org/10.1016/j.jvolgeores.2022.107526>.
- Rodriguez-Gonzalez, A., Fernandez-Turiel, J. L., Aulinas, M., Cabrera, M. C., Prieto-Torrell, C., Rodríguez, G. A., Guillou, H., Perez-Torrado, F. J., 2022. Lava deltas, a key landform in oceanic volcanic islands: El Hierro, Canary Islands. *Geomorphology* 416, 108427, <https://doi.org/10.1016/j.geomorph.2022.108427>.
- Salvador, A. (Ed.), 1994. *International stratigraphic guide: A guide to stratigraphic classification, terminology, and procedure* (No. 30). Geological Society of America.
- Troll, V. R., Carracedo, J. C., 2016. The geology of El Hierro. En: *The Geology of the Canary Islands*. Elsevier, pp. 43-99. <https://doi.org/10.1016/B978-0-12-809663-5.00002-5>.
- Villasante-Marcos, V., Pavón-Carrasco, F. J., 2014. Palaeomagnetic constraints on the age of Lomo Negro volcanic eruption (El Hierro, Canary Islands). *Geophysical Journal International* 199 (3), 1497–1514, <https://doi.org/10.1093/gji/ggu346>.

This article accompanies the following material:

- Static map: [10.22201/igg.25940694e.2025.2.113.44](https://doi.org/10.22201/igg.25940694e.2025.2.113.44)
 Interactive map: [10.22201/igg.25940694e.2025.2.113.45](https://doi.org/10.22201/igg.25940694e.2025.2.113.45)
 Supplementary material: [10.22201/igg.25940694e.2025.2.113.53](https://doi.org/10.22201/igg.25940694e.2025.2.113.53)